

Study of the $P^{31}(\alpha, d_{0,1})S^{33}$ Reactions at 18.7 MeV*†

B. B. SRIVASTAVA, S. W. COSPER,‡ AND O. E. JOHNSON

Department of Physics, Purdue University, Lafayette, Indiana

(Received 31 August 1966)

The 18.72-MeV differential cross sections for the $P^{31}(\alpha, d)S^{33}$ reactions leading to the ground and 0.841-MeV states of S^{33} have been measured from 15° to 170° at 5° intervals. The deuteron spectra were determined using a spectrometer configuration which incorporated an $E \times \Delta E$ mass identification system and an $(E, \Delta E)$ counter telescope consisting of two silicon surface-barrier detectors. The target was prepared by the thermal vacuum evaporation of red phosphorus ($650 \pm 12 \mu\text{g}/\text{cm}^2$) onto a thin Formvar film ($\sim 20 \mu\text{g}/\text{cm}^2$). In contrast to the well-defined oscillatory shape of the angular distribution associated with the transition to the 0.841-MeV state, that corresponding to the transition to the ground state has only washed-out undulations. The integrated cross sections for the ground and 0.841-MeV state reactions are $724 \pm 16 \mu\text{b}$ (16.9° – 171.3°) and $425 \pm 10 \mu\text{b}$ (17.0° – 171.3°), respectively. An analysis of the data in the distorted-wave Born approximation has been made in terms of a zero-range, knock-out model in which the initial (final) nuclear state is represented as a two-body system with a deuteron (alpha particle) bound to a Si^{29} core. Good agreement between the experimental and theoretical angular distributions was achieved. The analyses require a $2s_{1/2}$ state for the (d, Si^{29}) system representing the ground state of P^{31} , and $1d_{3/2}$ and $2s_{1/2}$ states for the (α, Si^{29}) system representing the ground and 0.841-MeV states of S^{33} , respectively. An interpretation of the experimental results on the basis of the dominant shell-model configurations for the states of P^{31} and S^{33} yields the conclusion that there is no enhancement of the transition in which the members of the transferred nucleon pair enter equivalent orbitals relative to that in which the nucleons enter nonequivalent orbitals.

I. INTRODUCTION

THE (α, d) reaction in light nuclei has been a subject of considerable interest principally because of the observed selectivity in the population of final nuclear states.^{1–7} Clearly, the understanding and characterization of this selectivity would enhance the utility of the (α, d) reaction as a spectroscopic tool.⁸ Toward this end Glendenning⁹ has presented a theory of direct two-nucleon transfer reactions formulated so that the way in which the structure of the nuclear states can influence the strength and multipolarity of the transition is shown. To date, the only (α, d) reactions which have been investigated using this theory are the

$C^{12}(\alpha, d)N^{14}$ transitions which were treated in the original report. It should also be noted that the latter study includes no intercomparisons between experimental and theoretical angular distributions. A fuller extension of this type of analysis in the distorted-wave Born approximation (DWBA) could only be made for cases where: (1) The structure of the nuclear states can be more or less reliably calculated; and (2) optical-model descriptions for both the entrance and exit channels are known to be reasonably adequate. Although there have been a large number of isolated measurements of (α, d) cross sections, the number of transitions for which the differential cross sections have been measured over a large angular range is quite small and corresponds to an even smaller number of light target nuclei, $A \leq 16$.^{2–7, 10–19} Up to the present time the (α, d) angular distributions have only been analyzed in terms of various plane-wave formulations. These analyses were performed on data corresponding to the

* Work supported in part by the U. S. Atomic Energy Commission.

† This report is based on part of a thesis submitted by B. B. Srivastava to the faculty of Purdue University in partial fulfillment of the requirements for the degree of Ph.D. in physics.

‡ Present address: University of California, Lawrence Radiation Laboratory, Berkeley, California.

¹ B. G. Harvey, J. Cerny, R. H. Pehl, and E. Rivet, Nucl. Phys. **39**, 160 (1962).

² B. G. Harvey, J. Cerny, R. H. Pehl, E. Rivet, and W. W. True, in *Direct Interactions and Nuclear Reaction Mechanisms* (Gordon and Breach Science Publishers Inc., New York, 1963), p. 974.

³ B. G. Harvey and J. Cerny, Phys. Rev. **120**, 2162 (1960).

⁴ J. Cerny, Ph.D. thesis, University of California Radiation Laboratory Report No. UCRL-9714, 1961 (unpublished).

⁵ E. Rivet, Ph.D. thesis, University of California Radiation Laboratory Report No. UCRL-11341, 1964 (unpublished) (Order No. 64-13084, University Microfilms Inc., Ann Arbor, Michigan).

⁶ R. H. Pehl, E. Rivet, J. Cerny, and B. G. Harvey, Phys. Rev. **137**, B114 (1965).

⁷ J. Cerny, B. G. Harvey, and R. H. Pehl, Nucl. Phys. **29**, 120 (1962).

⁸ A review and summary, with emphasis on spectroscopic aspects, of the available information concerning the deuteron transfer reactions, in general, and the (α, d) reaction, in particular, has been presented by D. A. Bromley in *Nuclear Spectroscopy with Direct Reactions, II. Proceedings*, edited by F. E. Throw (Argonne National Laboratory, Argonne, Illinois, 1964), Report No. ANL-6878, p. 353.

⁹ N. K. Glendenning, Phys. Rev. **137**, B102 (1965).

¹⁰ B. Zeidman and J. L. Yntema, Nucl. Phys. **12**, 298 (1959).

¹¹ H. R. Blieden, G. M. Temmer, and K. L. Warsh, Nucl. Phys. **49**, 209 (1963).

¹² G. Deconinck and G. Demortier, Phys. Letters **7**, 260 (1963).

¹³ G. Demortier, J. B. Dossin, G. A. Savariraj, and G. Deconinck, Ann. Soc. Sci. Bruxelles, Ser. I **77**, 81 (1963).

¹⁴ K. Ono and K. Kuroda, Phys. Rev. **117**, 214 (1960).

¹⁵ R. J. Silva, Ph. D. thesis, University of California Radiation Laboratory Report No. UCRL-8678, 1959 (unpublished).

¹⁶ S. V. Starodubtsev and K. V. Makaryunas, Dokl. Akad. Nauk SSSR **129**, 547 (1959) [English transl.: Doklady **4**, 1292 (1960)].

¹⁷ M. P. Konstantinova, E. V. Myakinin, A. M. Petrov, and A. M. Romanov, Zh. Eksperim. i Teor. Fiz. **43**, 388 (1962) [English transl.: Soviet Phys.—JETP **16**, 278 (1963)].

¹⁸ R. H. Pehl, Ph.D. thesis, University of California Radiation Laboratory Report No. URCL-10993, 1963 (unpublished) (Order No. 64-9070, University Microfilms, Inc., Ann Arbor, Michigan).

¹⁹ C. D. Zafiratos, Ph.D. thesis, University of Washington, 1962 (unpublished) (Order No. 62-6622, University Microfilms Inc., Ann Arbor, Michigan).

following target nuclei and incident alpha-particle energies: Li^6 at 10.15,¹⁶ 11.5,¹⁶ 13.2,¹⁶ 14.7,¹⁷ 43,¹⁰ and 48 MeV⁷; Li^7 at 48 MeV⁴; Be^9 at 48 MeV¹⁵; B^{10} at 3.80 MeV^{14,20}; C^{12} at 48 MeV⁸; N^{14} at 43¹⁰ and 46.5 MeV^{4,7}; and N^{15} at 46.5 MeV.⁴ While considerable effort has been directed with some success toward obtaining detailed descriptions of the states of very light nuclei, for these nuclei it is not at all clear that the elastic alpha-particle and deuteron cross sections may be even approximately characterized by the nuclear optical model. Until sufficient experimental information which meets the above criteria is available for detailed analysis, it might be argued that an intermediate step toward a fuller understanding of the (α, d) reaction could be made through studies involving DWBA analyses which are based on simpler and less detailed models. The recent demonstration of the adequacy of optical-model descriptions of the (α, α) and (d, d) reactions on P^{31} at 18.2²¹ and 9.8²² MeV, respectively, rendered the $\text{P}^{31}(\alpha, d)\text{S}^{33}$ reaction particularly convenient for this type of investigation. In the following sections are described the measurements of the $\text{P}^{31}(\alpha, d_0, 1)\text{S}^{33}$ reactions and analyses of the results in which the foregoing viewpoint was adopted.

II. EXPERIMENTAL

A description of the general arrangement of the Purdue University 37-in. cyclotron experimental area, the beam transport and analyzing systems, and the 30-in. scattering chamber has been presented elsewhere.²³

A. Target

The single phosphorus target used in this investigation was prepared by the thermal vacuum evaporation of red phosphorus onto a thin ($\sim 20 \mu\text{g}/\text{cm}^2$) Formvar film. The measured areal density of the phosphorus was $650 \pm 12 \mu\text{g}/\text{cm}^2$. Continuous monitoring of reaction particles emitted from the target at a fixed laboratory angle indicated that no change in target thickness occurred during the course of the measurements.

B. The Spectrometer System

The deuteron spectra were measured using a spectrometer configuration incorporating an $(E, \Delta E)$ counter telescope, a mass identification system, and a 256-channel pulse-height analyzer. A functional block diagram of the complete spectrometer system is presented in Fig. 1.

The counter telescope consisted of a ΔE counter, a transmission-mounted, fully depleted silicon surface-

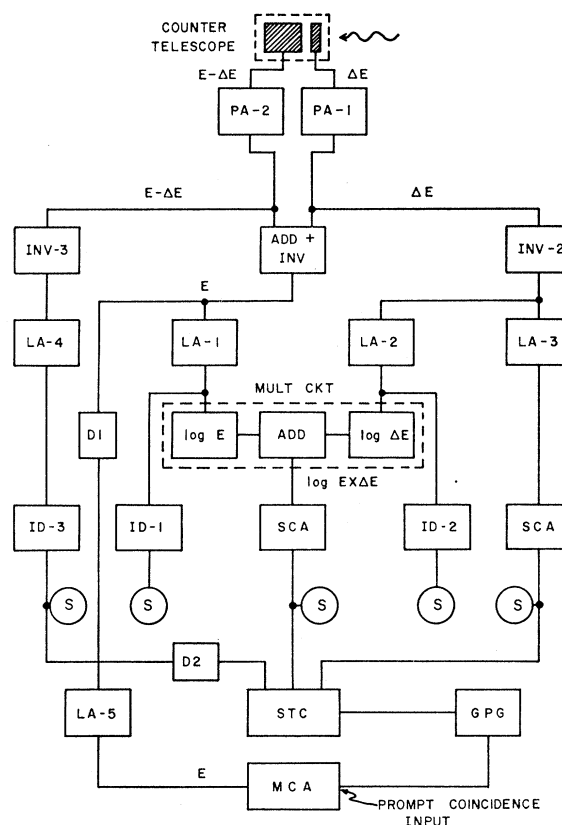


FIG. 1. A block diagram of the mass-discriminating spectrometer system. The functional component designations are as follows: PA—charge-sensitive preamplifier; INV—inverting circuit; ADD—linear addition circuit; LA—linear amplifier; $\log E$ and $\log \Delta E$ —logarithmic attenuators; ID—integral discriminator; SCA—single-channel differential discriminator; S—scaler; D1 and D2—variable lengths of delay cable (RG 65/U); STC—slow triple coincidence circuit ($\tau \approx 1.5 \mu\text{sec}$); GPG—gate pulse generator; and MCA—256-channel pulse-height analyzer.

barrier detector with a thickness of $40 \pm 2 \mu$ uniform to better than 6%, and an $(E, \Delta E)$ counter, a silicon surface-barrier detector with a maximum depletion depth of 720μ at 120-V bias. The detectors were preceded by a system of circular antiscattering baffles and defining apertures.

Since the general principles of operation of spectrometer configurations of the type shown schematically in Fig. 1 are well known, only a few experimental details concerning the system which was used in the present investigation will be given. Particle identification was accomplished by imposing both upper and lower limits on the ΔE and $\log(E \times \Delta E)$ pulses, a lower limit on the $(E, \Delta E)$ pulse, and judiciously adjusting the depletion depth of the $(E, \Delta E)$ detector. A pulse proportional to the full energy of each particle, the E pulse, was formed by electronically summing the $(E, \Delta E)$ and ΔE channels. The voltage-energy gains of the $(E, \Delta E)$ and ΔE channels were matched using the 6.047- and 6.086-MeV alpha-particle groups associated with the decay of Bi^{212}

²⁰ B. K. Jain and N. Sharma, Phys. Rev. **137**, B800 (1965).

²¹ B. T. Lucas, S. W. Cosper, and O. E. Johnson, Phys. Rev. **144**, B972 (1966).

²² B. T. Lucas and O. E. Johnson, Phys. Rev. **145**, B887 (1966).

²³ B. T. Lucas, S. W. Cosper, and O. E. Johnson, Phys. Rev. **133**, B963 (1964).

to within 1% at the output of the addition circuit. The over-all energy resolution of the system (FWHM) for the 8.780-MeV alpha-particle group from Po^{212} was 66 keV. The $\log(E \times \Delta E)$ pulse was formed using a circuit similar to that devised by Vincent and Kaine²⁴ in which the outputs of two logarithmic attenuators $\log E$ and $\log \Delta E$ are summed.

Because of the occurrence of numerous very strong proton groups throughout the energy region corresponding to the deuteron groups of interest, the principal experimental difficulty was the complete discrimination against protons while maintaining full detection efficiency for deuterons. The mass discrimination system used was inherently incapable of meeting this stringent requirement over an extended energy interval under the experimental circumstances which were encountered; consequently, only the angular distributions for the ground- and first-excited-state deuteron groups were measured. During the course of these measurements proton-rejection and deuteron-detection efficiencies were checked through the intercomparison of spectra obtained using various settings for the differential limits on the ΔE and $\log(E \times \Delta E)$ single-channel analyzers. The stability and alignment of the system were monitored using an extensive series of pulser checks.

In Fig. 2 is shown a portion of a spectrum obtained with the particle-identification circuitry adjusted such that the deuteron-detection efficiency was maintained in the energy region about d_0 and d_1 and the rejection of other reactions particles as complete as practicable (Curve A), and the corresponding one without mass discrimination (Curve B).²⁵ It should be noted that the curve representing the mass-discriminated spectrum has been scaled up by a factor of 10 for visual clarity. The relationship between the two spectra as shown in Fig. 2 is typical of the experimental situation over the entire angular range.

C. Alpha-Particle Beam and Experimental Geometry

The energy of the alpha particles incident on the phosphorus target was 18.72 MeV with an inherent rms spread of 60 keV. The energy spread due to finite target thickness and target orientation was nominally 100 keV. The beam cross section perpendicular to its direction was circular in shape with a 5/64-in. diam. Beam currents of about $5\text{--}15 \times 10^{-9}$ A were used in these measurements.

The target-detector geometry yielded a detector

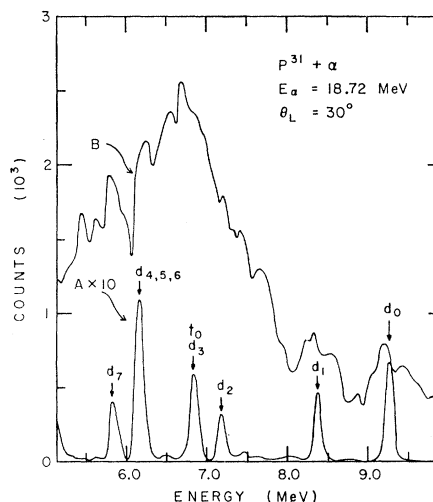


FIG. 2. A comparison of experimental charged-particle spectra associated with the bombardment of P^{31} with 18.72-MeV alpha particles as observed at a laboratory angle of 30° with and without mass discrimination, Curves A and B, respectively. The identification of the particle groups associated with the $P^{31}(\alpha, d_N)S^{33}$ and $P^{31}(\alpha, t_N)S^{33}$ reactions was based mainly on reaction kinematics using information from Ref. 25. It should be noted that the discriminated spectrum has been scaled up by a factor of 10. The spectrometer system was adjusted for the highest proton-rejection efficiency which was consistent with full deuteron-detection efficiency for d_0 and d_1 at all angles. Although other deuteron groups appear to be well resolved, the concurrence of other particles due to imperfect discrimination and/or the lack of full deuteron-detection efficiency over substantial portions of the angular range covered made it impossible to derive valid cross sections for (α, d) transitions to states higher than the 0.841-MeV state of S^{33} .

azimuthal acceptance angle of 2.3° and a nominal solid angle of 0.001 sr with respect to the beam-spot center.

III. EXPERIMENTAL RESULTS

The 18.72-MeV (α, d) differential cross sections for those reactions which leave S^{33} in its 0.841-MeV and ground states are shown in Figs. 3 and 4, respectively. The bars on the experimental points represent probable errors based on counting statistics. The probable systematic error in the absolute differential cross sections due to uncertainties in target thickness, beam current integration, and experimental geometry is estimated to be about 15%. Only first-order finite geometry corrections have been applied to the experimental data.

The shapes of these two angular distributions not only differ in detail but have one distinct difference in general character. In contrast to the excited-state cross section which has a well-defined oscillatory structure, that corresponding to the ground-state reaction has only washed-out undulations.

The integrated cross sections are $724 \pm 16 \mu\text{b}$ ($16.9^\circ\text{--}171.3^\circ$) and $425 \pm 10 \mu\text{b}$ ($17.0^\circ\text{--}171.3^\circ$) for the ground and 0.841-MeV state transitions, respectively.

²⁴ C. H. Vincent and D. Kaine, IRE Trans. Nucl. Sci. NS-9, 327 (1962).

²⁵ Unless otherwise specified, the level structure and individual level properties proposed for P^{31} and S^{33} in the following compilation will be assumed: P. N. Endt and C. Van der Leun, Nucl. Phys. 34, 1 (1962). In those instances where revised and/or more detailed information is essential to the discussion, appropriate bibliographical references will be made.

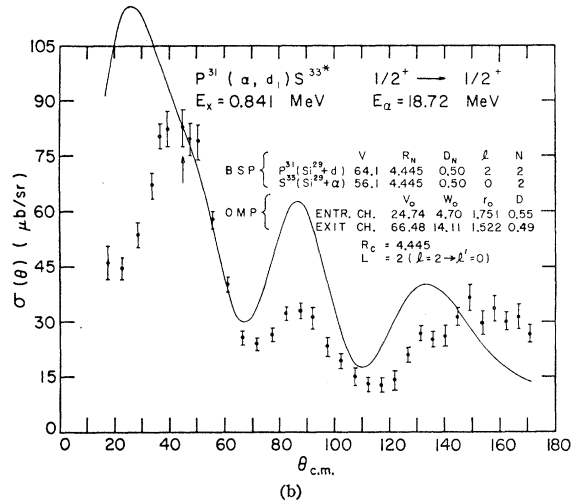
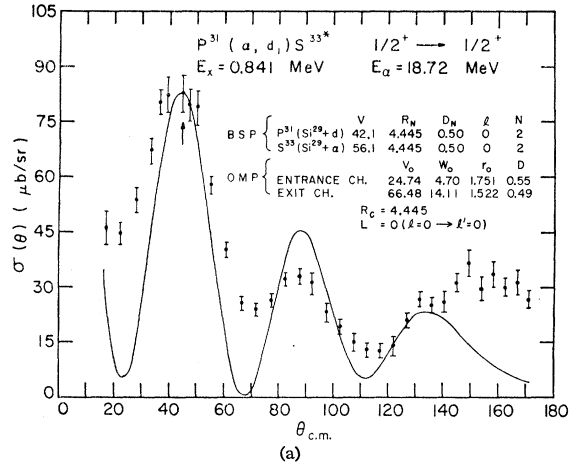


FIG. 3. The experimental differential cross section for the $P^{31}(\alpha, d_1)S^{33*}$ reaction (solid circles) and a comparison of the best-fitting DWBA, knock-out cross sections (solid curves) assuming either a $2s$ (3a) or a $2d$ (3b) orbital for the (Si^{29}, d) system representing the ground state of P^{31} together with a $2s$ orbital for the (Si^{29}, α) system representing the first excited state of S^{33} . Included in each section of the figure are the incident alpha-particle energy E_α ; the final state excitation energy E_x ; the spin and parties of the nuclear states; the bound-state parameters BSP; the entrance- and exit-channel optical-model parameters OMP; the cutoff radius R_c ; and the angular momentum transfer L . The only quantities adjusted in the fitting procedures were the cutoff radius, the radial quantum numbers N , and a normalization constant. The point of normalization is at 45° and is indicated by an arrow.

IV. ANALYSIS

A. General

A distorted-wave Born-approximation analysis of the present data has been made within the framework of a zero-range, knock-out formalism due to Tobocman²⁶ using the direct-reaction code developed and described by Gibbs *et al.*²⁷ Since complete descriptions of the

²⁶ W. Tobocman, *Theory of Direct Nuclear Reactions* (Oxford University Press, London, 1961).

²⁷ W. R. Gibbs, V. A. Madsen, J. A. Miller, W. Tobocman, E. C. Cox, and L. Mowry, Natl. Aeron. Space Admin. Tech. Note No. TN-D2170 (1964).

formalism and computational details have been presented elsewhere, the reiteration of formulas will be minimized.

In Fig. 5 is presented a schematic representation of the knock-out reaction along with some details concerning the initial and final states, and the allowed values of the angular momentum transfer. The DWBA amplitude for the knock-out reaction characterized in Fig. 5 is

$$A_{ad}(\mathbf{K}_\alpha, \mathbf{K}_d) = \langle \Phi_{dF}^{(-)}(\mathbf{K}_d) \varphi_d \varphi_F | V_{d\alpha} + V_{dC} - \bar{V}_{dF} | \Phi_{\alpha I}^{(+)}(\mathbf{K}_\alpha) \varphi_\alpha \varphi_I \rangle, \quad (1)$$

where $\Phi_{\alpha I}^{(+)}$ and $\Phi_{dF}^{(-)}$ are the optical-model (OM) wave functions for the relative motion of the particles in the entrance and exit channels, respectively; each φ is the internal wave function of the entity denoted by the subscript; V_{dC} and $V_{d\alpha}$ are the potentials taken to describe the interaction of the deuteron with the core and the alpha particle; and \bar{V}_{dF} is the appropriate OM potential for the exit channel. In the development used to make the present analysis the interaction potential is simplified by assuming that

$$V_{dC} - \bar{V}_{dF} = 0, \quad (2)$$

and by making the zero-range approximation

$$V_{d\alpha} \sim \delta(\mathbf{r}_\alpha - \mathbf{r}_d). \quad (3)$$

For the entrance channel, the OM parameters were taken from among the sets derived by Lucas *et al.*²¹ through analyses of their measured cross sections for 18.2-MeV alpha-particle scattering from P^{31} . They were made using a Saxon-Woods, four-parameter potential

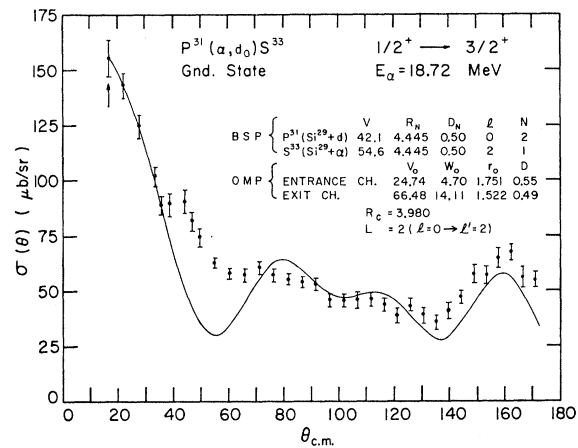


FIG. 4. The experimental differential cross section for the $P^{31}(\alpha, d_0)S^{33}$ reaction (solid circles) and the best-fitting DWBA, knock-out cross section (solid curve), assuming a $2s_{1/2}$ state for the (Si^{29}, d) system representing the ground state of P^{31} and a $1d_{3/2}$ state for the (Si^{29}, α) system representing the ground state of S^{33} . The general format for this figure is the same as that of Fig. 3. The point of normalization is at 16.9° and is indicated by an arrow.

of the form

$$U(r) = -(V_0 + iW_0)/(e^x + 1), \quad (4)$$

where

$$x = (r - r_0 A^{1/3})/D, \quad (5)$$

together with a Coulomb potential corresponding to a uniformly charged sphere of radius $1.2A^{1/3}$ F. The exit-channel description requires a set of OM parameters corresponding to elastic deuteron scattering from S^{33} at about 8 MeV. This information was not available, therefore, the single set of OM parameters derived by Cosper²⁸ from 9.5-MeV elastic deuteron scattering from P^{31} using the potential described above was employed.²⁹ The sets of OM parameters used in the present study are listed in Table I.

As indicated in Fig. 5 the initial (final) nucleus is taken to be a bound two-body system consisting of a deuteron (alpha particle) and a core, Si^{29} in its ground state. The bound-state wave functions φ_I and φ_F are calculated assuming a two-body interaction characterized by a Coulomb potential for a uniformly charged sphere and a *real* nuclear potential with a Saxon-Woods shape. The radius parameter R_N in the Saxon-Woods form factor and the Coulomb potential were both set equal to 4.445 F for the initial and final states,³⁰ that is, were not used as adjustable parameters in the fitting procedures. Furthermore, the diffusivity parameter in the Saxon-Woods form factor was assigned a fixed value of 0.500 F. Having fixed these parameters, the determination of the real well depth requires that the binding energy, relative orbital angular momentum, and number of nodes in the radial wave function be specified. In each case the binding energy was calculated from the known masses and excitation energy for the nuclear state.

TABLE I. The optical-model parameters corresponding to elastic deuteron and alpha-particle scattering from P^{31} which were adopted for use in the distorted-wave analyses of the present investigation.

Reaction	Energy (MeV)	Set No.	V_0 (MeV)	W_0 (MeV)	D (F)	r_0 (F)
$(\alpha, \alpha)^a$	18.2	1	24.74	4.70	0.550	1.751
		2	40.62	8.13	0.440	1.807
		3	88.01	10.91	0.432	1.765
$(d, d)^b$	9.5	1	66.48	14.11	0.492	1.522

^a See Ref. 21.

^b See Ref. 28.

²⁸ S. W. Cosper, Ph.D. thesis, Purdue University, 1965 (unpublished).

²⁹ A subsequent report (see Ref. 22) based on the analyses of new experimental data for the (d, d) reaction on P^{31} at 9.8 MeV lists three sets of OM parameters, including one whose values are very close to those used in the present study. Moreover, this latter set was judged to yield one of the better fits to the elastic-scattering data and the best fit to the inelastic-scattering data when used in a DWBA analysis.

³⁰ Radius parameters for P^{31} and S^{33} were calculated taking $R_N = 1.44A^{1/3}$ F, but because the difference between these two values is much smaller than the grid size used in calculating the radial integrals, their mean value of 4.445 F was adopted for both nuclei.

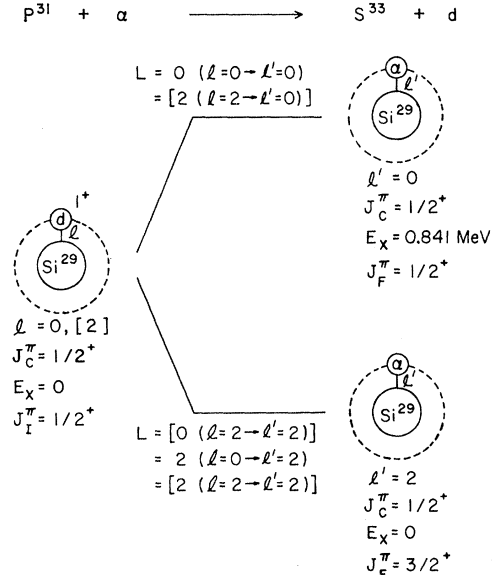


FIG. 5. A graphic representation of the knock-out reaction and some pertinent information concerning the two-body systems assumed to represent the nuclear states of interest in P^{31} and S^{33} . The information shown includes: the excitation energy of the nuclear state, E_x ; the intrinsic angular momentum and parity of each constituent of the two-body systems, J_N^π ; the relative orbital angular momenta allowed by the selection rules for each two-body system, l and l' ; and the values of the angular momentum transfer, L , consistent with the selection rules. The square brackets indicate the values of L which are excluded by the experimental data.

The total angular momentum of the initial and final nuclear states may be written in terms of the intrinsic angular momentum of the core and extracore entity, and their relative orbital angular momentum, that is,

$$\mathbf{J}_I = \mathbf{J}_C + \mathbf{J}_d + \mathbf{I} \quad \text{and} \quad \mathbf{J}_F = \mathbf{J}_C + \mathbf{I}'. \quad (6)$$

The admissible values of l and l' are dictated by the above equations and parity considerations. The angular-momentum transfer,

$$\mathbf{L} \equiv \mathbf{J}_F + \mathbf{J}_d - \mathbf{J}_I, \quad (7)$$

can take on values consistent with the three conditions:

$$|l - l'| \leq L \leq l + l', \quad (8)$$

$$L \leq J_F + J_d + J_I, \quad (9)$$

and

$$(-1)^L = (-1)^{l+l'}. \quad (10)$$

The final expression for the differential cross section involves an incoherent sum over the allowed values of L , and each term corresponding to a particular L value involves a coherent sum over those values of l and l' which lead to that L value. Within the formalism itself there is nothing to preclude the possibility of multiple values for l and/or l' . This type of multiplicity would in general lead to an ambiguity in the depth of the potential well through the l -dependent centrifugal term in the radial equation, provided there is not a set of radial

quantum numbers, one for each allowed l value, which yield the same well depth. In the absence of an accidental degeneracy, the circumstance of multiple values for l is physically irreconcilable within the literal context of this model. For the final states of interest only single values of l' are implied by the selection rules—2 and 0 for the ground- and first-excited states of S^{33} , respectively. On the other hand, for the initial state, the ground state of P^{31} , both $l=0$ and 2 are admitted. It can be categorically stated that for the nuclear radii adopted in the present study and for the binding energies of the states of interest a degeneracy, approximate or otherwise, does not occur for reasonable values of the radial quantum numbers. Accordingly, it will be assumed that only a single l value is associated with ground state of P^{31} .

At this point it is essential to outline the general philosophy adopted in making the intercomparisons between the theoretical and experimental angular distributions. The analysis was performed in a manner in strict adherence to the spirit of the distorted-wave theory, that is, no adjustments of the entrance- and exit-channel OM parameters were made in the fitting procedures. In attempting to reproduce the experimental cross sections, parameter values were sought which yielded the best agreement over the *entire* angular range. In making the subjective judgements as to the goodness of fit, more weight was given to the reproduction of the shape of the angular distribution than its magnitude.

B. Procedures and Results

As indicated in Sec. IV-A, some criteria for the selection of one of the two allowed l values for the ground state of P^{31} was essential. The selection was based on the relative quality of agreement between the resulting theoretical and experimental angular distributions for various choices of the radial quantum numbers as the cutoff radius R_C was varied from 1.0 to 8.0 F. The (α, d_1) angular distribution was chosen for use in making this comparison because it has a well-defined shape with pronounced structure. Moreover, for this reaction each of the two choices of l for the P^{31} ground state leads to a single value for the angular momentum transfer. The initial investigation was made taking the No. 1 sets of OM parameters (see Table I) for the entrance and exit channels. In Fig. 3 is shown a comparison of those (α, d_1) theoretical cross sections which were judged to be in closest correspondence with the experimental results for these two choices of l . The values of all parameters, both fixed and adjusted, are shown in each section of Fig. 3. The experimental point at 45° , indicated by the arrow, is the point of normalization. It is evident that the $l=0$ curve gives the better representation of the experimental data. In the course of these initial analyses it was found that the general character of the (α, d_1) angular distribution

clearly required that $R_C \geq R_N$, since for $R_C < R_N$ the oscillatory structure of the theoretical cross section tended to weaken and wash out. As a consequence of this, when the best value of R_C was determined to be equal to R_N , the quality of the fit was found to be insensitive to the values of the radial quantum numbers. The justification of the assignment of $N=2$ for both the initial and final nuclear states in the (α, d_1) reaction follows.

Having removed the ambiguity in the l value of the initial nuclear state, the fitting of the (α, d_0) angular distribution was undertaken using a procedure in which again only the cutoff radius, the radial quantum numbers, and a normalization constant were adjusted. As suggested above the washed-out structure of the experimental angular distribution required $R_C < R_N$; and the shape of the theoretical angular distribution depended strongly on the values of the radial quantum numbers. The theoretical angular distribution which was judged to best fit the experimental results is shown in Fig. 4. The general format of Fig. 4 is the same as that of Fig. 3. It will be noted that the radial quantum numbers 2 and 1 are required for the ground states of P^{31} and S^{33} , respectively. Thus the states of the two-particle systems representing the ground states of P^{31} and S^{33} were determined to be $2s_{1/2}$ and $1d_{3/2}$, respectively. On the basis of a literal physical interpretation of this two-body nuclear model, it is reasonable to require very nearly the same bound-state potential-well depths for the final nuclear state in both the (α, d_0) and (α, d_1) reaction. To achieve this end, it was necessary to assign $N=2$ to the 0.841-MeV state of S^{33} , that is, a $2s_{1/2}$ state for the (Si^{29}, α) two-body system.

Identical procedures were followed using the No. 2 and 3 sets of OM parameters (see Table I) for the entrance channel. For each set it was found that the best fit resulted for the (α, d_1) angular distribution when an s orbital was assumed for the (Si^{29}, d) bound system. It was noted that although the positions of the maxima and minima could be reproduced with a cutoff radius equal to or slightly larger than the nuclear radius ($R_C=4.755$ and 4.445 F for OM parameter sets Nos. 2 and 3, respectively), as the real OM potential-well depth increased both the ratio of the magnitudes of the second and third maxima in the cross section to that of the first maxima increased and the magnitudes of the backward-angle minima increased. While the quality of the best fits achievable with sets Nos. 2 and 3 are definitely inferior to that found for the No. 1 set in the case of the (α, d_1) angular distribution, the unsuitability of sets Nos. 2 and 3 became manifest in attempting to fit the (α, d_0) angular distribution.

V. DISCUSSION

The close correspondence between each experimental angular distribution and that calculated on the basis of the extremely simple model described above is some-

what surprising. It is particularly interesting to note that within the framework of the Tobocman knock-out model the difference in the general character of the two angular distributions—oscillatory in contrast to washed out—appears to be correlated with whether the cutoff radius is taken to be equal to or less than the nuclear radius. To date there has been no evidence presented which unambiguously identifies the dominant mechanism in the (α, d) reaction on light nuclei as stripping or knock-out. The fact that a knock-out model seems to fit the data cannot be construed as relevant in this connection, since as Austern emphasizes,³¹ all the zero-range, direct-reaction calculations yield expressions for angular distributions of essentially the same type although the magnitudes of the cross sections may differ. However, it should be noted that if the quality of the fits was taken as evidence that the model used for the nuclear states has some physical basis, then an interpretation from the point of view of a nuclear-cluster model would be most natural. To date no cluster-model analyses of any of the states of P^{31} and S^{33} have been reported. In view of the limited number of angular distributions analyzed it is not unlikely that both the quality of the fits and the correlation between the size of the cutoff radius and general character of the angular distribution are fortuitous.

In an early experimental study concerning the selectivity of the (α, d) reaction with light nuclei in populating final states Cerny⁴ found some experimental results which suggested the possibility of the occurrence of the following systematics: (1) The two stripped nucleons prefer to be captured into equivalent shell-model states, and, when that is not possible, prefer to enter adjacent states; and (2) transitions to final state configurations involving one or more excited nucleons, so that their formation would require core excitation in addition to two-nucleon transfer are relatively weak. At the time of the study the only experimentally well-established exceptions to these observations were the $Li^6(\alpha, d)Be^8$ reactions populating the ground, 2.90-, and 11.4-MeV states of Be^8 .⁴ The results of subsequent measurements by Pehl *et al.*⁶ concerning (α, d) transi-

tions to the 5.10- and 5.83-MeV states of N^{14} do not follow the above systematics. The results of the present investigation may also be brought to bear on this point through the use of the shell-model description of the states of P^{31} and S^{33} provided by Glaudemans *et al.*,³² in which an inert Si^{28} core was assumed with two-particle interactions of the outer nucleons in the $2s_{1/2}$ and $1d_{3/2}$ shells. The most dominant configurations for the relevant states are: the P^{31} ground state,

$$68\%_O[\pi(2s_{1/2})^1; \nu(2s_{1/2})^2] + 29\%_O[\pi(2s_{1/2})^1; \nu(1d_{3/2})^2];$$

the S^{33} ground state,

$$62\%_O[\pi(2s_{1/2})^2; \nu(2s_{1/2})^2(1d_{3/2})^1] \\ + 16\%_O[\pi(1d_{3/2})^2; \nu(2s_{1/2})^2(1d_{3/2})^1] \\ + 13\%_O[\pi(2s_{1/2})^2; \nu(1d_{3/2})^3];$$

and the S^{33} 0.841-MeV state,

$$73\%_O[\pi(2s_{1/2})^2; \nu(2s_{1/2})^1(1d_{3/2})^2] \\ + 13\%_O[\pi(1d_{3/2})^2; \nu(2s_{1/2})^1(1d_{3/2})^2] \\ + 11\%_O[\pi(2s_{1/2})^1(1d_{3/2})^1; \nu(2s_{1/2})^2(1d_{3/2})^1].$$

For each of the S^{33} states two of the three dominant configurations may be obtained from the two most dominant configurations of the P^{31} ground state by the simple addition of the two nucleons without exciting the core. Of particular significance to the present discussion is the fact that the nucleons would go into nonequivalent orbitals and equivalent orbitals in the ground and 0.841-MeV state transitions, respectively. The ratio of the reduced experimental cross sections $\sigma_{\text{exp}}(2J_I+1)/(2J_F+1)$ for the transition to the 0.841-MeV state to that for the transition to the ground state, is 1.17, which is inconsistent with the systematic (1) above.

ACKNOWLEDGMENTS

We are grateful to Dr. B. T. Lucas for many helpful discussions. We wish to thank Professor D. J. Tendam and the accelerator crew for their diligence in the operation of the cyclotron and assistance in its maintenance throughout this investigation.

³¹ N. Austern in *Selected Topics in Nuclear Theory* (International Atomic Energy Agency, Vienna, 1963), p. 30.

³² P. W. M. Glaudemans, G. Wiechers, and P. J. Brussaard, *Nucl. Phys.* **56**, 529 (1964); **56**, 548 (1964).